Two-Dimensional NMR Studies of the Antimicrobial Peptide NP-5†

Alvin C. Bach, II,‡,‖ Michael E. Selsted,§ and Arthur Pardi*,‡

Department of Chemistry, Rutgers, The State University of New Jersey, New Brunswick, New Jersey 08903, and Departments of Medicine and Pathology, The Center for Health Science, University of California, Los Angeles, Los Angeles, California 90024

Received October 10, 1986; Revised Manuscript Received January 6, 1987

ABSTRACT: Nearly complete proton resonance assignment of the rabbit antimicrobial peptide NP-5 has been made from two-dimensional NMR data taken at a single temperature. The assignment procedure involved acquisition of phase-sensitive double-quantum-filtered correlation spectra, relayed coherence-transfer spectra, total correlation (homonuclear Hartmann–Hahn) spectra, double- and triple-quantum spectra, and nuclear Overhauser effect spectra. The combination of these complementary experiments simplified and accelerated resonance assignment of the peptide. Individual assignments were made at 20 °C for all amide and C^{α} protons in the peptide, and for all nonlabile side-chain protons on 26 of the 33 amino acid residues in NP-5. Analysis of the proton–proton nuclear Overhauser effect connectivities, the slowly exchanging amide protons, and the proton chemical shifts in NP-5 indicates that the peptide has a stable, ordered structure in solution. These data also indicate that residues 19–29 in NP-5 are involved in an antiparallel β-sheet that has a hairpin conformation.

Neutrophil peptide 5 (NP-5)[1] belongs to a recently characterized family of naturally occurring broad-spectrum antimicrobial peptides termed defensins (Selsted et al., 1985a,b). These low molecular weight cationic peptides form part of the oxygen-independent antimicrobial mammalian defense system. Six rabbit peptides (Selsted et al., 1985a), three human peptides (Selsted et al., 1985b), and one guinea pig peptide have been isolated and shown to possess activity against Gram-positive and Gram-negative bacteria (Selsted et al., 1984), fungi (Lehrer et al., 1985a), and herpes simplex virus (Lehrer et al., 1985b). These homologous peptides are all cysteine- and arginine-rich, are 29–34 residues in length, and have 8 conserved residues in the whole family. In addition to the biochemical studies, a member of the defensin family is being studied by X-ray crystallography (Westbrook et al., 1984).

Application of 2D NMR techniques has led to nearly complete resonance assignment of the ^{1}H NMR spectra of a number of proteins (Wuethrich et al., 1982; Wagner & Wuethrich, 1982a; Wemmer & Kallenbach, 1983; Zuiderweg et al., 1983). Once proton resonance assignments have been made, it is possible to use information derived from 2D NMR spectra to probe the secondary (Wuethrich et al., 1984; Pardi et al., 1984; Wagner et al., 1986) and tertiary (Kaptein et al., 1985; Havel & Wuethrich, 1985; Williamson et al., 1985; Bruenger et al., 1986) structure of the protein in solution. The rate-limiting step in using NMR data to generate three-dimensional structures of proteins in solution is generally resonance assignment of the ^{1}H NMR spectrum. Therefore, it is important to develop strategies for accelerating the assignment process. In this paper we describe a procedure for making resonance assignments in proteins that involves application of a number of recently developed 2D NMR techniques. The improved assignment procedure consists of acquisition of two-dimensional double- and triple-quantum spectra, two-dimensional total correlation spectra, and relayed coherence-transfer spectra, in addition to standard DQF-COSY and NOESY spectra. 2D spectra involving the exchangeable amide protons were acquired in 90% H_2O by using DQ and modified NOESY pulse sequences where loss of any cross-peaks near the water signal was avoided. Application of the techniques outlined here can enormously facilitate the sequential resonance assignment process and also leads to greater confidence in the resonance assignments once they have been made. This improved methodology for making sequential resonance assignments in proteins is illustrated by assignment of the antimicrobial peptide NP-5. Structural information on NP-5 derived from these NMR data is also discussed.

Materials and Methods

Rabbit NP-5 was isolated and purified as previously described (Selsted et al., 1984). Samples were prepared at a concentration of 7 mM peptide in 10 mM sodium phosphate buffer, pH 3.5. The peptide was dissolved in 0.5 mL of 90% H_2O/10% D_2O for the H_2O experiments. For the D_2O experiments the peptide was dissolved in 99.8% D_2O (Stohler Isotopes) and the labile protons were exchanged by repeated lyophilization and redissolution in D_2O. The final D_2O NMR sample was dissolved in 0.5 mL of 99.996% D_2O (Stohler Isotopes) under nitrogen. The pH (or pD) of both samples

† This work was supported in part by grants from the Searle Scholars Program of the Chicago Community Trust 85-C110, NIH GM35801, a Henry Rutgers Research Fellowship, and Biomedical Research Support Grant PHS RR 07058-20 to A.P. and by NIH AI22931 and the Office of Naval Research N00014-86-K-0525 to M.E.S. The 400-MHz NMR spectrometer was purchased with partial support from NSF Grant CHEM-8300444. This is Publication No. 123 of the Collaborative California Universities–Mycology Research Unit.

‡ Rutgers, The State University of New Jersey.

‖ Present address: Medical Products Department, E. I. du Pont, Wilmington, DE 19898.

§ University of California, Los Angeles.

[1] Abbreviations: NP-5, neutrophil peptide 5 from rabbit; NMR, nuclear magnetic resonance; 1D, one dimensional; 2D, two dimensional; COSY, two-dimensional correlation spectroscopy; NOE, nuclear Overhauser effect; NOESY, two-dimensional nuclear Overhauser effect spectroscopy; DQF-COSY, two-dimensional double-quantum-filtered correlation spectroscopy; TOCSY, two-dimensional total correlation spectroscopy; FID, free induction decay; TQ, two-dimensional triple-quantum spectroscopy; DQ, two-dimensional double-quantum spectroscopy; RELAYED-COSY, two-dimensional relayed coherence-transfer spectroscopy; HOHAHA, two-dimensional homonuclear Hartmann–Hahn spectroscopy; ppm, parts per million; rf, radio frequency; AMX, weakly coupled three-spin system.

0006-2960/87/0426-4389$01.50/0

was adjusted to pH 3.50 ± 0.04, this value being the uncorrected pH meter reading measured at room temperature. For spectra containing the slowly exchanging amide protons in NP-5, the sample was dissolved in buffer, adjusted to pH 3.5, and lyophilized. It was then redissolved in D_2O at pH 3.5, and a double-quantum-filtered COSY (Piantini et al., 1982; Shaka & Freeman, 1983) experiment was immediately acquired.

The 2D NMR spectra were recorded on a Varian XL-400 spectrometer operating at 400 MHz with a sample temperature of 19.8 ± 0.5 °C. All spectra were acquired in the phase-sensitive absorption mode with quadrature detection in both dimensions (Mueller & Ernst, 1978; States et al., 1982). Quadration detection during the evolution time, t_1, was accomplished by separately storing two FIDs for each t_1 value. The second FID of each pair had the phase of all pulses prior to the t_1 period shifted by $90°/n$ relative to their phase in the first FID, where n is the quantum number of the coherence that evolves during t_1. This corresponds to a 90° phase shift for all the 2D spectra discussed here except for the double-quantum and triple-quantum experiments, which required 45° and 30° phase shifts, respectively. The method of "phase pulses" (Guittet et al., 1985) was used to obtain phase shifts that are not multiples of 90°. The carrier frequency was centered on the water signal, and a recycle delay of 1.0–1.5 s was used in all spectra. The spectral width was 4500 Hz in the acquisition period, t_2, in all 2D spectra, and 4500 Hz in t_1 for all spectra except the triple-quantum spectroscopy experiment, which had a spectral width of 6750 Hz in t_1. All 2D spectra were collected in the following form: 512 or 1024 complex points in t_2, 256–512 complex FIDs in t_1, and 64–160 transients for each FID. For each spectrum both time domain data sets were multiplied by a 0–90° phase-shifted sine bell window function and then zero filled to 1024 complex points before Fourier transformation. For the multiple-quantum spectra, the spectral width was set such that the spectra were folded in ω_1 in order to improve digital resolution. These spectra were unfolded by appropriate shifting of the 2D data matrix after Fourier transformation. The quadrature pairs of FIDs for the first t_1 value in all 2D spectra were mutliplied by 0.5 after Fourier transformation along t_2 in order to eliminate t_1 ridge artifacts (Otting et al., 1986). All data processing was done on a VAX 11/750 or micro VAX II computer using the FORTRAN program FTNMR kindly provided by Dr. D. Hare.

2D NMR Experiments in D_2O. Continuous low-power irradiation of the residual water signal was applied during the recycle time in all D_2O spectra. The DQF-COSY spectrum (Piantini et al., 1982; Shaka & Freeman, 1983) and the NOESY spectrum (Macura & Ernst, 1980) with 200-ms mixing time were recorded by standard methods. The MLEV-17 pulse sequence (Bax & Davis, 1985) was used to drive the coherence transfer in the TOCSY or HOHAHA experiment (Braunsweiler & Ernst, 1983; Davis & Bax, 1985) on NP-5. A 7.8-kHz rf field was used for the MLEV-17 spin lock pulse whereas a normal full-power pulse was used for the 90° pulse. The spin lock field was applied for 72 ms so that coherence could be transferred through a number of protons on the amino acid side chains (Bax & Davis, 1985; Summers et al., 1986). The triple-quantum spectrum (Wokaun & Ernst, 1977; Rance & Wright, 1985) was recorded with a multiple-quantum excitation time of 71 ms, which corresponds to optimal excitation between protons with J couplings of 7 Hz.

2D NMR Experiments in H_2O. Continuous low-power irradiation of the H_2O signal was applied during the recycle time in all 2D spectra in H_2O except for the NOESY spectra. For all H_2O spectra a fifth-order polynomial base-line correction routine was applied to the amide region of the frequency domain spectra after Fourier transformation and phase correction in t_2, but prior to the t_1 transform. This procedure eliminates modulation of the base line caused by the tail of the water signal and enormously reduces "t_1 noise" produced by variation of the phase, and the degree of suppression, of the water signal for different t_1 values.

The DQF-COSY and RELAYED-COSY (Eich et al., 1982; Wagner, 1983) spectra in H_2O were acquired by standard methods. A double-quantum spectrum in H_2O (Wokaun & Ernst, 1977; Wagner & Zuiderweg, 1983) was acquired with a multiple-quantum excitation time of 71 ms, which corresponds to optimal excitation between protons with J couplings of 7 Hz. NOESY spectra with mixing times of 200 and 400 ms were acquired with no water irradiation where the water signal was reduced by application of a binomial 1331 water suppression 90° pulse (Hore, 1983) as the detection pulse. This pulse sequence has the form (Schwartz & Cutnell, 1983):

$$[-t_0-90°-t_1-90°-\tau_m-90°(1331)-t_2-]_n$$

where t_0 is the recycle time and τ_m the mixing time during which the NOE develops. The transverse magnetization of the water signal excited by the first two 90° pulses in this NOESY pulse sequence relaxes during the long mixing times used here. This method of acquiring NOESY spectra in H_2O makes it possible to detect all NOEs involving the exchangeable amide protons in the molecule, even those NOEs for C^α protons directly under the water signal.

Results

Strategy for Sequential Resonance Assignment. Techniques for resonance assignment of proteins have been previously described by Wuethrich and co-workers (Wuethrich et al., 1983; Neuhaus et al., 1985) and will be only briefly discussed here. The first step in the assignment procedure is to identify resonances belonging to the same amino acid residue. This information can be obtained from a variety of experiments that probe through-bond J-coupling connectivities between protons belonging to the same spin system. The pattern of these connectivities in the 2D spectrum is then used to classify the spin system to a specific amino acid type, or to a class of amino acid types. In addition to J-coupling information, through-space NOE information allows identification of certain amino acid types. For example, in aromatic amino acids NOEs are used to connect the backbone and C^β protons in an individual spin system to their aromatic protons. Once identification of amino acid type, or class of amino acid types, has been made, NOE connectivities are used to "walk" from one residue to its nearest-neighbor residues in the amino acid sequence. Statistical studies of protein crystal structures show that most short proton–proton distances arise from intraresidue interactions or nearest-neighbor residue interactions (Billeter et al., 1982). The majority of the short distances between neighboring residues involve an amide proton and the amide, C^α, or C^β protons on the neighboring residue. The following notation is commonly used to describe these distances (Wuethrich et al., 1984):

$$d_{\alpha N} = d(C^\alpha H_i, NH_{i+1}) \qquad d_{NN} = d(NH_i, NH_{i+1})$$
$$d_{\beta N} = d(C^\beta H_i, NH_{i+1})$$

The information on amino acid type, along with NOEs between neighboring residues, is then combined with the known

Table I: Complete Sequential Connectivity Diagram for NP-5

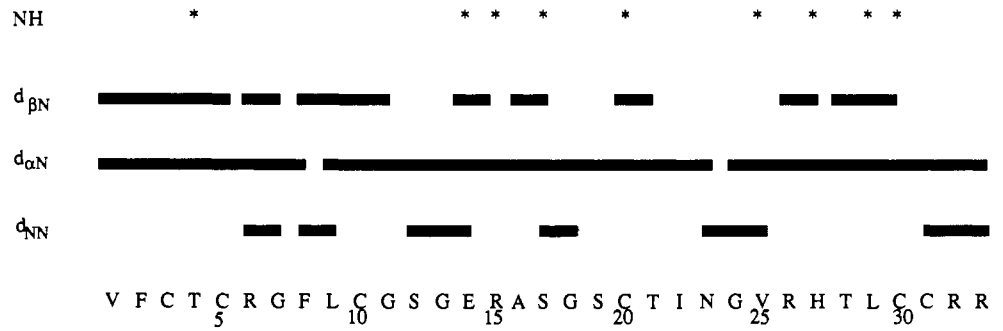

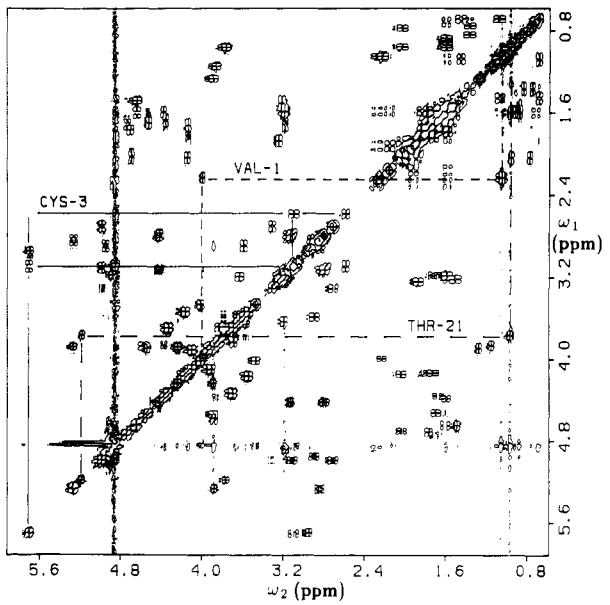

FIGURE 1: Contour plot of the ^1H DQF-COSY spectrum of NP-5 in D_2O. Proton–proton J-coupling connectivities are shown for the Val-1, Cys-3, and Thr-21 spin systems. Positive and negative contours are plotted in the figure.

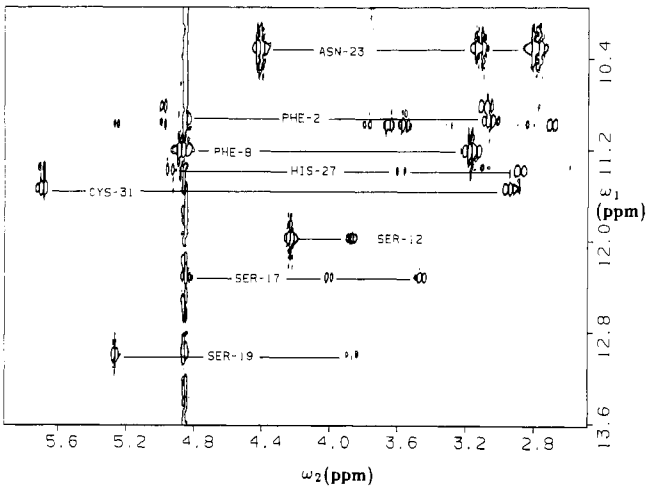

FIGURE 2: Contour plot of the C^α and C^β proton region of the TQ spectrum of NP-5 in D_2O. Triple-quantum frequencies are plotted along ω_1 and single-quantum frequencies along ω_2. Positive and negative contour levels are plotted in the figure. The horizontal lines connect the C^α protons to the C^β protons in the same spin system. The Phe-2, Phe-8, Ser-12, Ser-17, Ser-19, Asn-23, His-27, and Cys-31 spin systems are illustrated.

amino acid sequence to give sequential resonance assignment of the protein. Once complete resonance assignments have been made, it is possible to use NOE distance data (Wuethrich et al., 1982; Wemmer & Kallenbach, 1983; Williamson et al., 1984), J-coupling constant data (Pardi et al., 1984), and chemical shift information (Bundi & Wuethrich, 1979; Pardi et al., 1983) to generate three-dimensional structures of proteins in solution (Williamson et al., 1985; Kaptein et al., 1985; Havel & Wuethrich, 1985; Bruenger et al., 1986).

Spin-System Assignments and Identification of Amino Acid Type in NP-5. Table I gives the amino acid sequence of NP-5 and shows that NP-5 contains several amino acid types with unique spin systems, including Ala-16, five Arg residues, Glu-14, five Gly residues, Ile-22, two Leu residues, three Thr residues, and two Val residues. The peptide also contains 13 "AMX spin systems" (Wider et al., 1982) consisting of Asn-23, six Cys residues, His-27, two Phe residues, and three Ser residues. The method used to identify amino acid type in NP-5 involved acquisition of three 2D NMR experiments in D_2O; a DQF-COSY experiment, a TQ experiment, and a TOCSY experiment. The DQF-COSY experiment gives connectivities between directly coupled protons (Piantini et al., 1982; Shaka & Freeman, 1983). Figure 1 shows a contour plot of a phase-sensitive absorption mode DQF-COSY spectrum of NP-5. The assignment of the amino acid spin systems on Val-1, Cys-3, and Thr-21 are illustrated in the figure. In DQF-COSY spectra the cross-peaks have antiphase character, and the sign and multiplet patterns of individual cross-peaks facilitated the identification of spin-coupling partners in crowded regions of this spectrum. A large number of amino acid spin systems were partially or completely assigned from this spectrum.

The major limitation in using DQF-COSY spectra to analyze J-coupling connectivities arises from overlap of resonances in different spin systems. This overlap often prevents unambiguous assignment of resonances to a specific spin system. One method for resolving these ambiguities is to use multiple-quantum spectroscopy (Wokaun & Ernst, 1977; Bodenhausen, 1981; Rance & Wright, 1985). Many ambiguities involving assignment of the C^α and C^β protons in NP-5 were resolved by acquisition of a 2D triple-quantum experiment. This experiment selects for three-quantum coherence during the evolution time which is then transferred to single-quantum coherence on the individual spins. Such information is extremely helpful in mapping connectivities involving a C^α proton and its two neighboring C^β protons. Figure 2 shows a contour plot of a TQ experiment on NP-5. An example of how a TQ experiment can enormously facilitate spin-system assignments is illustrated by the assignment of Ser-12 and Ser-19 in NP-5. The C^α protons of Ser-12 and Ser-19 have chemical shifts of 4.24 and 5.27 ppm, respectively, while all four C^β protons have chemical shifts of 3.88 ppm. Initial inspection of the DQF-COSY spectrum indicated that all these resonances originated from one AMX spin system with the C^α proton at 5.27 ppm and the two C^β protons at 4.24

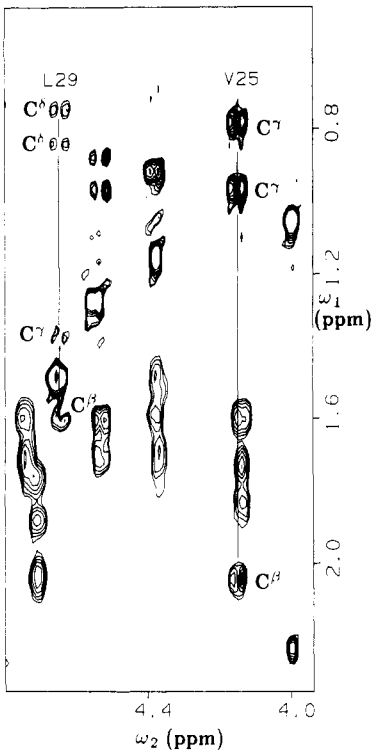

FIGURE 3: Contour plot of the ^1H TOCSY spectrum of NP-5 in D_2O. $C^{\alpha}H$ chemical shifts appear along the ω_2 axis while the C^{β}, C^{γ}, and C^{δ} chemical shifts appear along the ω_1 axis. For Val-25, connectivities from the $C^{\beta}H$ and C methyl protons to the C^{α} proton are shown. Similarly, for Leu-29, connectivities from all the side-chain protons to the C^{α} proton are shown.

and 3.88 ppm. Only one $C^{\alpha}H$–$C^{\beta}H$ cross-peak was observed in the DQF-COSY spectrum, but this is often seen in an AMX spin system where one $J_{\alpha\beta}$ is small. Analysis of the TQ spectrum in Figure 2 immediately reveals that these resonances originate from two AMX spin systems (which were subsequently assigned to Ser-12 and Ser-19). For each of these AMX spin systems, both C^{β} protons have degenerate chemical shifts, so no $C^{\beta}H$–$C^{\beta}H$ cross-peaks are observed in the DQF-COSY spectrum. Such degeneracies are obvious in the TQ spectrum where cross-peaks occur at the three-quantum frequency, $\delta_{\alpha} + \delta_{\beta 1} + \delta_{\beta 2}$, in ω_1. If the single-quantum frequencies of only two of the three protons are known, the third can be calculated from the measured triple-quantum frequency. In this way, the TQ experiment resolved a number of ambiguities in the DQF-COSY spectrum and also provided independent confirming evidence for many assignments made from the DQF-COSY spectrum.

For amino acid residues with spin systems larger than an AMX system, it is sometimes difficult to follow connectivities past the C^{β} protons to the C^{γ} or C^{δ} protons because of spectral overlap. Techniques for relaying magnetization between protons that are not directly coupled are extremely useful for overcoming such difficulties. A RELAYED-COSY experiment (Eich et al., 1982; Wagner, 1983) performs a single relay of magnetization beyond the directly coupled protons. Extension of this technique to multiple relays is limited in proteins because of relaxation during the multiple coherence-transfer times. A more powerful method for obtaining multiple relays was proposed by Ernst and co-workers and involves application of an isotropic mixing technique (Brausweiler & Ernst, 1983). This TOCSY or HOHAHA (Davis & Bax, 1985) experiment gives quite efficient multiple relay of magnetization throughout a spin system. Figure 3 shows a portion of the TOCSY spectrum on NP-5 where a MLEV-17 sequence (Bax & Davis, 1985) was used for the spin lock pulse. This figure shows a contour plot of the phase-sensitive version of this experiment where the cross-peaks have predominantly absorption mode character with a minor dispersion component (Davis & Bax, 1985). Connectivities between the C^{α} proton and the C^{β} and C^{γ} protons on Val-25, and between the C^{α} proton and the C^{β}, C^{γ}, and C^{δ} protons on Leu-29, are illustrated in the figure. This isotropic mixing experiment gave much more efficient transfer of magnetization than the RELAYED-COSY experiment on NP-5 (data not shown). Detailed analysis of this isotropic mixing spectrum by itself and in combination with the DQF-COSY and TQ data allowed complete assignment of many extended amino acid spin systems in NP-5.

The spin-system assignments of aromatic protons in NP-5 were made from analysis of 1D spectra and the DQF-COSY spectrum. Further analysis of the D_2O NOESY spectrum allowed connectivities to be made from these aromatic protons to their C^{β} protons on the two Phe residues and His-27. Once all the spin-system assignments to amino acid types were complete, it was possible in certain cases to assign these resonances to specific amino acids in the peptide. For example, the assignment of Ile-22 and His-27 was accomplished because both residues have unique spin-system types in NP-5. These amino acid residues provide valuable starting points for sequential resonance assignment of the rest of the peptide.

The sequential resonance assignment procedure in proteins centers on the amide protons. Therefore, it is critical to attach the amide protons to the spin systems assigned above. Figure 4A shows the $C^{\alpha}H$–NH "fingerprint" region of a DQF-COSY spectrum of NP-5 in H_2O. Continuous selective preirradiation of H_2O signal was used to suppress the large water signal for the spectra in H_2O. The amount of power needed to effectively suppress the H_2O signal in this DQF-COSY spectrum also saturated 12 C^{α} protons near the water signal. A DQ spectrum in H_2O (with the same irradiation power level) was acquired to gain information on these C^{α} protons. As discussed by Otting and Wuethrich (1986), it is possible to excite double-quantum $C^{\alpha}H$–NH coherence in a DQ experiment even when this single-quantum $C^{\alpha}H$ frequency is saturated. Figure 4B shows a DQ spectrum of NP-5 in H_2O where the 2D data matrix has been shifted to remove the NH frequency in ω_1 (Zuiderweg, 1986). This shifting allows the DQ spectrum to be presented in the same form as the DQF-COSY spectrum. Comparison of spectra A and B of Figure 4 shows that the $C^{\alpha}H$–NH cross-peaks that were bleached out by water saturation in the DQF-COSY spectrum are readily observed in the DQ spectrum. Combining both these spectra, 31 of 32 $C^{\alpha}H$–NH cross-peaks in NP-5 are observed and are identified in Figure 4. The only $C^{\alpha}H$–NH cross-peak missing was for Leu-29, which was subsequently identified in the NOESY spectra. The absence of this cross-peak probably means that the $J_{\alpha NH}$ coupling constant is small for this residue.

When there are degeneracies of $C^{\alpha}H$ chemical shifts in the protein, it is not always possible to assign a particular amide proton to a specific spin system. To overcome such ambiguities, a RELAYED-COSY experiment in H_2O was acquired on NP-5. This experiment gives intraresidue $C^{\beta}H$–NH connectivities in the molecule. This information was combined with the spin-system assignments to clear up ambiguities that were present in the DQF-COSY or DQ data sets. At this point in the assignment procedure, all the amide protons were connected to specific spin systems in the molecule. These spin systems were also classified to a specific amino acid type, or class of amino acid types. The next step involved the use of NOEs between neighboring residues to "walk" down the

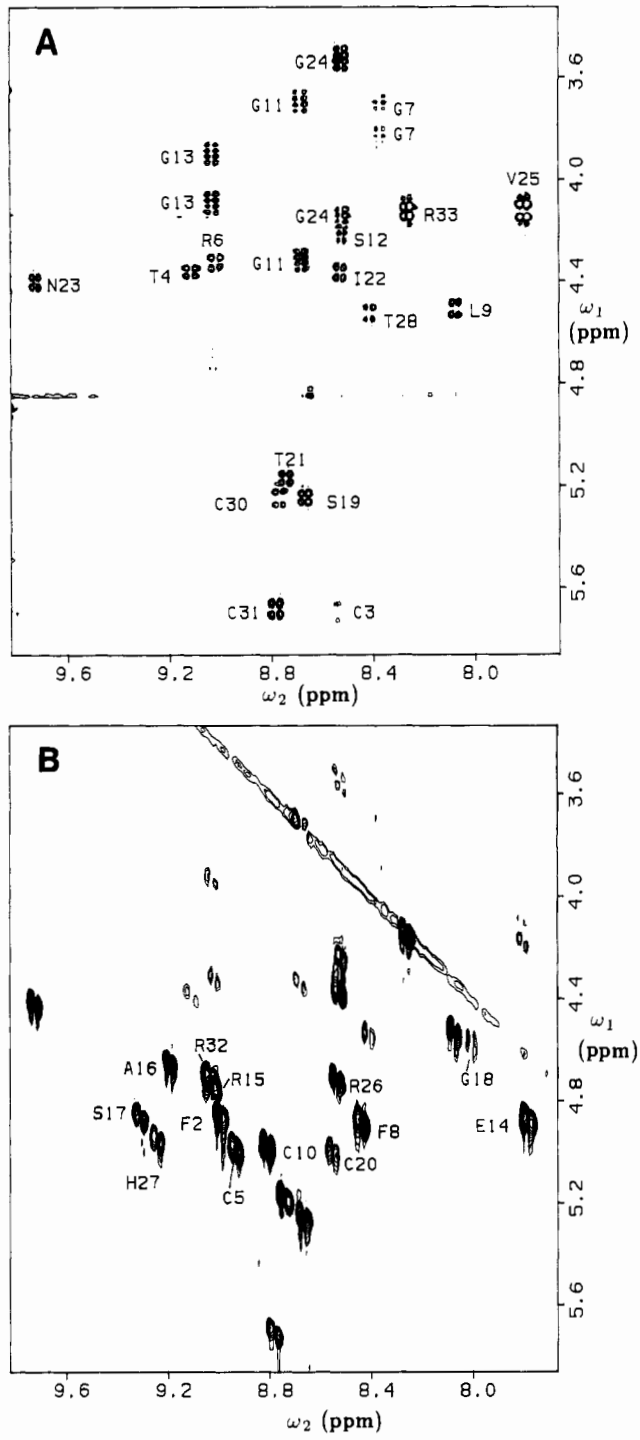

FIGURE 4: Contour plots of the $C^{\alpha}H$–NH fingerprint region of NP-5 in H_2O: (A) DQF-COSY spectrum; (B) DQ spectrum. The DQ spectrum was shifted to the same scale as the DQF-COSY spectrum by subtraction of the NH frequency in ω_1 (see text). Positive and negative contours are plotted in both spectra. $C^{\alpha}H$–NH cross-peaks are labeled with standard single-letter amino acid abbrevatiations. Thirty-one of the 32 $C^{\alpha}H$–NH cross-peaks are visible in these spectra. The only resonances that are labeled in the DQ spectrum (spectrum B) are those that were not observed in the DQF-COSY spectrum because of water irradiation (see text).

peptide backbone and make sequential assignment of the molecule.

Sequential Resonance Assignment of NP-5. A NOESY spectrum in H_2O was acquired on NP-5 to search for NOEs between protons on neighboring amino acid residues. Figure 5 shows a portion of a NOESY spectrum in H_2O where the H_2O signal was reduced by application of a water suppression pulse as the final pulse in the pulse sequence. This spectrum

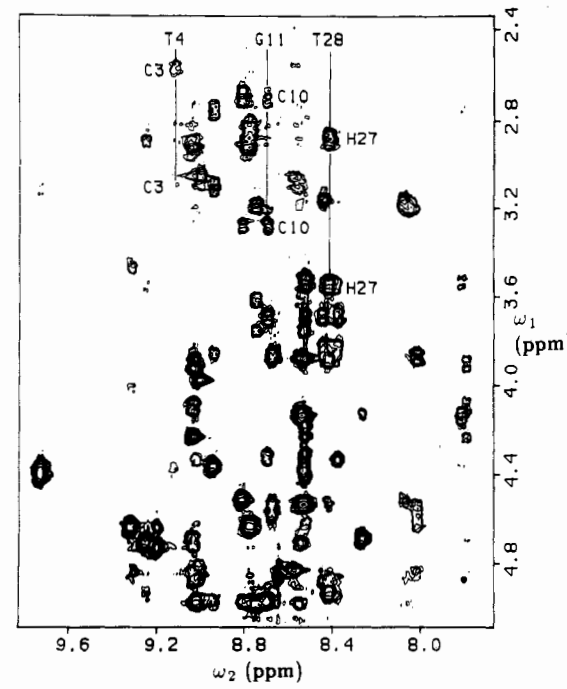

FIGURE 5: Contour plot of a portion of the 400-ms ^1H NOESY spectrum of NP-5 in H_2O showing several NOE connectivities from amide protons to the C^{β} protons of the preceding residue ($d_{\beta N}$). Three examples where $d_{\beta N}$ connectivities are observed between an amide proton and both C^{β} protons of the preceding residue are illustrated: T4 to C3, G11 to C10, and T28 to H27. Standard single-letter amino acid abbreviations are used.

has equivalent signal to noise to a NOESY spectrum taken with water irradiation (data not shown), but no cross-peaks near the water signal at 4.8 ppm were lost from preirradiation at the water frequency. Thus all NOEs involving amide protons were obtained from a single NOESY spectrum. Sequential assignments were then made by combining this NOESY spectrum with the DQ and DQF-COSY spectra in H_2O.

For NP-5 the sequential resonance assignment started at a number of places in the amino acid sequence. These starting points included Ile-22 and His-27, both of which have unique spin-system types in NP-5. Other useful starting points centered on the two Val and two Phe residues. The amide proton on one of the Phe residues showed an NOE to the C^{α}, C^{β}, and C^{δ} protons on a Val residue. The only Val–Phe sequence in NP-5 is Val-1–Phe-2. These assignments were supported by the fact that no $C^{\alpha}H$–NH cross-peak was observed for this Val residue, confirming that it was the amino-terminal residue. This result immediately led to the assignment of Val-25 and Phe-8, which were then used as additional starting points in the sequential assignment. As previously discussed (Wagner & Zuiderweg, 1983), a DQ spectrum in H_2O is extremely useful for selecting amide protons on glycine residues because of their distinct $C^{\alpha 1}H$–$C^{\alpha 2}H$ double-quantum frequency. Four of the five glycine amide and C^{α} protons were identified by this procedure in the DQ spectrum. When sequential assignments from these glycine residues were traced out, an AMX-Gly-AMX-Gly connectivity pattern was observed. Inspection of the NP-5 sequence shows that this pattern only occurs for the Cys-Gly-Ser-Gly sequence on residues 10–13.

Figure 6 shows an example of how the $d_{\alpha N}$ connectivities given in Table I were identified in NP-5. A combined DQF-COSY (and DQ)/NOESY diagram is shown where the $d_{\alpha N}$ connectivities from Phe-2 to Phe-8 are identified. Starting on the DQF-COSY spectrum with the $C^{\alpha}H$–NH J-coupling connectivity on Phe-8, the connectivity proceeds at constant

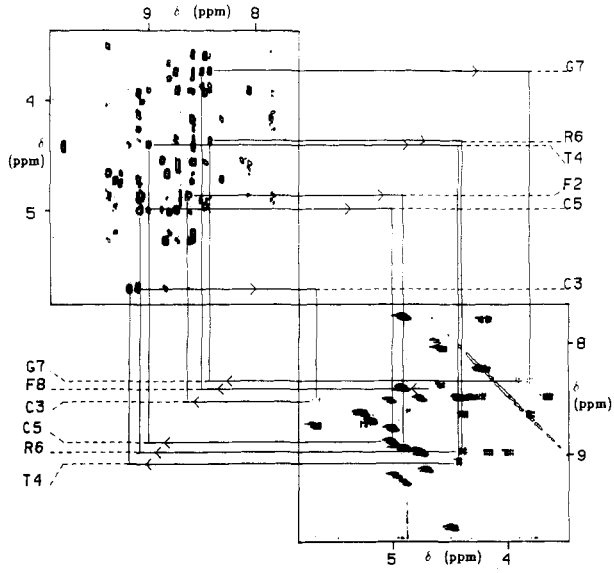

FIGURE 6: Combined DQF-COSY (and DQ)/NOESY connectivity diagram for sequential resonance assignment showing NOEs between amide protons and C^{α} protons of the preceding residue ($d_{\alpha N}$). The upper left corner contains the fingerprint region of the 200-ms NOESY experiment on NP-5. The lower right-hand corner contains the DQF-COSY and DQ spectra shown in Figure 4. The two spectra have been overlayed so that all the observed $C^{\alpha}H$–NH cross-peaks are shown in this figure. The lines and arrows indicate connectivities between residues Phe-8 to Phe-2. The arrow in the lower right-hand spectra indicates the start of this $d_{\alpha N}$ connectivity. Chemical shifts of the amide protons are annotated in the lower left corner, while the chemical shifts of the C^{α} protons are given in the upper right. Standard single-letter amino acid abbreviations are used.

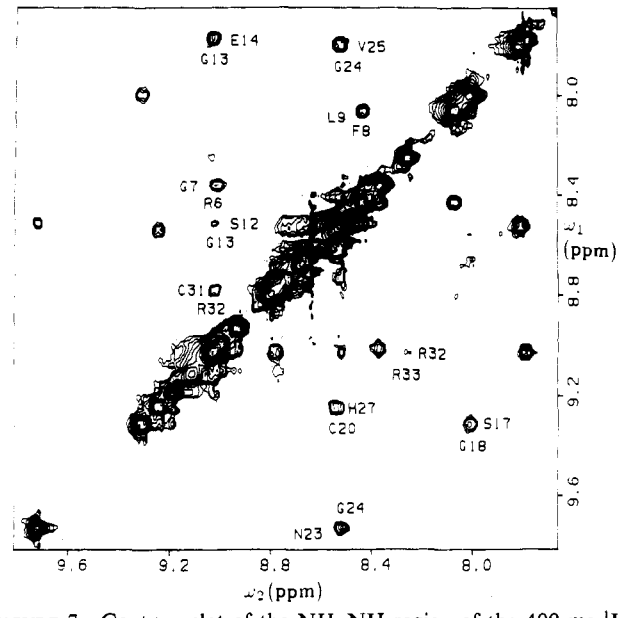

FIGURE 7: Contour plot of the NH–NH region of the 400-ms ^1H NOESY spectrum of NP-5 in H_2O. Cross-peaks from individual residues are labeled with their standard single-letter amino acid abbreviations. Five stretches of short d_{NN} connectivities are observed: R6–G7, F8–L9, S12–G13–E14, S17–G18, N23–G24–V25, and C31–R32–R33. One nonsequential NH–NH NOE is observed: C20 to H27.

NH chemical shift to the NOESY spectrum, where a cross-peak is observed to a C^{α} proton on Gly-7. This connectivity then proceeds to the DQF-COSY spectrum, where the $C^{\alpha}H$–NH J-coupling connectivity on Gly-7 is identified. The connectivity continues in this manner until Phe-2. The other $d_{\alpha N}$ connectivities observed in NP-5 were identified by similar analysis.

Table II: Chemical Shifts, δ, for the Assigned Proton Resonances of NP-5 at 20 °C, in 10 mM Sodium Phosphate, pH 3.5[a]

amino acid residue	NH	$C^{\alpha}H$	$C^{\beta}H$	others
Val-1		4.01	2.24	$C^{\gamma}H_3$ 1.06, 1.06
Phe-2	8.99	4.85	3.06, 3.06	ring 7.25
Cys-3	8.57	5.71	3.10, 2.59	
Thr-4	9.11	4.38	3.86	$C^{\gamma}H_3$ 1.15
Cys-5	8.94	4.99	3.08, 2.78	
Arg-6	9.01	4.37	1.68, 1.68	$C^{\gamma}H$ 1.52; $C^{\delta}H$ 3.23
Gly-7	8.36	3.84		
		3.69		
Phe-8	8.45	4.88	3.18, 3.18	ring 7.35
Leu-9	8.07	4.53	1.71, 1.56	$C^{\gamma}H$ 1.61; $C^{\gamma}H_3$ 0.98, 0.88
Cys-10	8.80	4.99	3.31, 2.72	
Gly-11	8.68	4.33		
		3.71		
Ser-12	8.52	4.24	3.88, 3.88	
Gly-13	9.02	4.11		
		3.91		
Glu-14	7.78	4.88	2.28	$C^{\gamma}H$ 1.58
Arg-15	9.01	4.73	1.72, 1.65	$C^{\gamma}H$ 1.60; $C^{\delta}H$ 3.19
Ala-16	9.19	4.66	1.49	
Ser-17	9.31	4.85	4.02, 3.47	
Gly-18	8.00	4.57		
		3.88		
Ser-19	8.66	5.27	3.88, 3.88	
Cys-20	8.55	5.00	3.64, 3.20	
Thr-21	8.74	5.19	3.77	$C^{\gamma}H_3$ 0.97
Ile-22	8.52	4.39	1.61	$C^{\gamma}H$ 1.47, 1.09; $C^{\beta}H_3$ 0.72 $C^{\delta}H_3$ 0.69
Asn-23	9.72	4.43	3.13, 2.80	
Gly-24	8.52	4.17		
		3.54		
Val-25	7.80	4.15	2.04	$C^{\gamma}H_3$ 0.96, 0.78
Arg-26	8.54	4.71	1.77	
His-27	9.24	4.95	3.60, 2.90	C2H 8.69; C4H 6.43
Thr-28	8.41	4.54	3.89	$C^{\gamma}H_3$ 1.28
Leu-29	8.52	4.65	1.61	$C^{\gamma}H$ 1.38; $C^{\delta}H_3$ 0.85, 0.76
Cys-30	8.76	5.27	2.94, 2.83	
Cys-31	8.77	5.69	2.96, 2.96	
Arg-32	9.03	4.70	2.03, 2.03	$C^{\gamma}H$ 1.88; $C^{\delta}H$ 3.25
Arg-33	8.26	4.14	1.84, 1.73	$C^{\gamma}H$ 1.60; $C^{\delta}H$ 3.20

[a] The chemical shifts, δ, have errors of ±0.03 ppm and are relative to the H_2O or HOD resonance that resonates at 4.85 ppm relative to sodium 3-(trimethylsilyl)propionate-*2,2,3,3-d*$_4$ under these conditions. Where no numbers are given in the column, individual resonance assignments were not obtained.

A large number of $d_{\beta N}$ connectivities were observed in NP-5 and aided the sequential assignment. Figure 5 shows several of these connectivities, including NOEs from the amide protons on residues Thr-4, Gly-11, and Thr-28 to the C^{β} protons on residues Cys-3, Cys-10, and His-27, respectively. The other $d_{\beta N}$ connectivities identified in NP-5 are given in Table I.

Figure 7 shows the NH–NH region of the NOESY spectrum of NP-5 in H_2O from which d_{NN} connectivities were identified. As seen in the figure and Table I, no long stretches of d_{NN} connectivities were observed in NP-5. Extension of these and other NOE connectivities gives the complete connectivity patterns for NP-5 listed in Table I. The proton chemical shifts for NP-5 at 20 °C are listed in Table II.

Discussion

Sequential Assignment Methodology. The basic principles underlying the sequential resonance assignment procedure in proteins by 2D NMR have not changed since its introduction by Wuethrich and co-workers (Wuethrich et al., 1983). However, since that time there has been tremendous development of 2D NMR techniques which can simplify and accelerate the assignment procedure. For example, acquisition of absorption-mode phase-sensitive 2D NMR spectra gives enormously improved resolution over absolute value mode

spectra (States et al., 1982; Marion & Wuethrich, 1983). Absorption-mode presentation also makes it possible to use the sign and multiplet patterns of cross-peaks to distinguish weak cross-peaks from noise and to sort out J-coupling connectivities in crowded regions of the spectrum (Neuhaus et al., 1985; Boyd & Redfield, 1986). A crucial step in the resonance assignment of a protein is the acquisition of 2D spectra in H_2O. The standard approach involves continuous low-power irradiation of the water signal during the 2D experiment (Wider et al., 1983). Such irradiation can also lead to saturation of protein resonances, and loss of information from these protons can seriously impede the assignment process. A different approach was used here to assign NP-5 and consisted of acquisition of 2D spectra at a single temperature employing pulse sequences that avoid loss of cross-peaks near the water signal. For probing $C^{\alpha}H$–NH J-coupling connectivities in proteins, a DQ spectrum acquired with water irradiation gives all $C^{\alpha}H$–NH cross-peaks (Otting & Wuethrich, 1986) even if the $C^{\alpha}H$ single-quantum frequency is saturated. This procedure enormously facilitated analysis of the $C^{\alpha}H$–NH fingerprint region in NP-5. For acquisition of NOESY spectra in H_2O it is possible to use water suppression pulse sequences, in place of water irradiation, to reduce the large water signal (Schwartz & Cutnell, 1983). For NP-5 this method allowed observation of all NOEs involving amide protons from a single spectrum, with no loss of cross-peaks at or near the H_2O frequency.

NP-5 Structure. Table I also shows that there are nine "slowly exchanging" amide protons in NP-5. These protons were found to exchange with half-lives of 1–10 days at 5 °C, pH 3.5. Observation of such slowly exchanging amide protons indicates that they are either buried, not accessible to solvent, and/or involved in intramolecular hydrogen bonds (Wagner & Wuethrich, 1982b). The presence of these slowly exchanging amide protons also indicates a certain degree of non-random-coil structure in the molecule. Stretches of slowly exchanging amide protons are seen in helical regions of a protein (Wagner & Wuethrich, 1982b; Englander & Kallenbach, 1984; Wand et al., 1986), whereas a pattern of alternating residues with slowly exchanging protons might be expected for an isolated strand of β-sheet. Analysis of these slowly exchanging protons indicates that NP-5 possesses some ordered, reasonably stable structure in solution.

Another indication that NP-5 has non-random-coil structure in solution comes from analysis of the proton chemical shifts in the molecule. The difference between a proton chemical shift in a protein and its random-coil chemical shift (McDonald & Phillips, 1969; Bundi & Wuethrich, 1979) represents the "conformation-dependent" chemical shift (Pardi et al., 1983). Comparison of Table II with the random-coil amino acid chemical shifts (Bundi & Wuethrich, 1979) shows that there are a number of sizable conformation-dependent chemical shifts in NP-5. For example, no amide protons have chemical shifts greater than 8.8 ppm in random-coil amino acids, whereas there are 11 amide protons with chemical shifts between 8.9 and 9.8 ppm in NP-5. Similarly, no C^{α} protons have chemical shifts greater than 4.8 ppm in the random coil whereas there are 13 C^{α} protons with chemical shifts between 4.85 and 5.75 ppm in NP-5. Large positive conformation-dependent chemical shifts on amide and C^{α} protons in proteins have been proposed to originate from protons involved in short intramolecular hydrogen bonds (Wagner et al., 1983). Thus qualitative analysis of the proton chemical shifts in NP-5 also supports the conclusion that NP-5 forms an ordered, non-random-coil structure in solution.

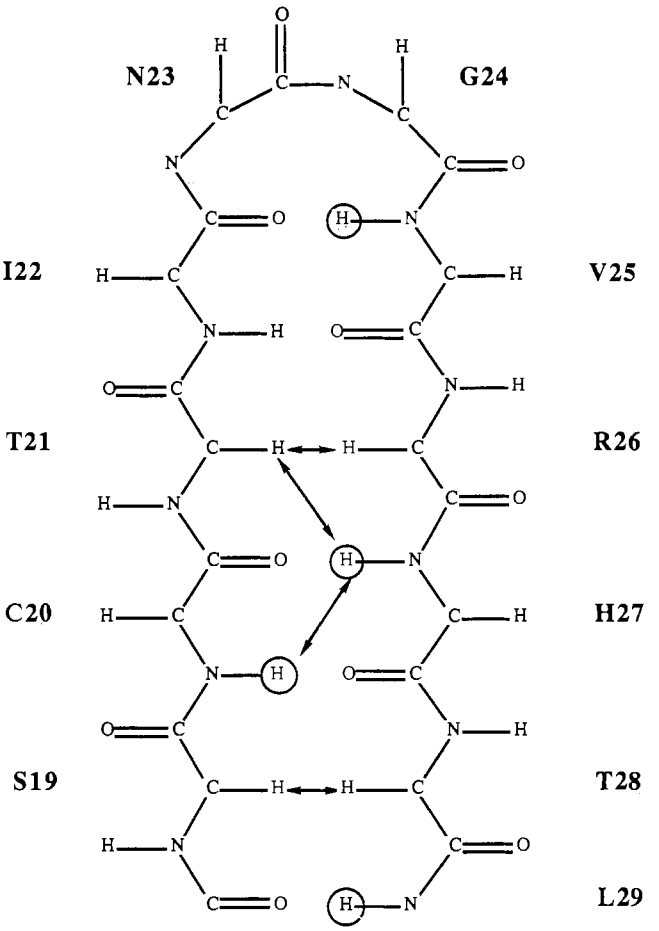

FIGURE 8: Schematic diagram of the antiparallel β-sheet structure involving residues 19–29 in NP-5. The amide protons that exchange slowly with D_2O are circled in the figure (see text). Arrows indicate cross-strand NOEs that are observed between the backbone C^{α} and amide protons.

Once complete resonance assignments have been made in a protein, distance information derived from NOESY spectra can be used to generate its three-dimensional structure in solution (Wuethrich et al., 1982, 1984). Statistical studies of X-ray crystal structures show that there are correlations between d_{NN}, $d_{\alpha N}$, and $d_{\beta N}$ connectivities and regular secondary structure in proteins (Wuethrich et al., 1984). Table I shows the NOE connectivity diagrams in NP-5. A detailed analysis of all the NOE connectivities will be presented elsewhere, but a number of qualitative structural conclusions can be made from the data presented here. There are no long stretches of d_{NN} connectivities in NP-5. The absence of such a pattern indicates that NP-5 has little or no helical secondary structure (Wuethrich et al., 1984). The d_{NN} connectivities that are observed in NP-5 probably arise from turns in the molecule (Wuethrich et al., 1984; Wagner et al., 1986). Thus, preliminary analysis of the sequential NOE connectivities indicates that NP-5 has little α-helical secondary structure but does have a number of tight turns. This lack of helical secondary structure is consistent with the results from circular dichroism studies on NP-5 (M. E. Selsted, unpublished results).

In addition to the sequential NOE connectivities, a large number of NOEs between protons on nonneighboring residues were observed in NP-5. Figure 8 illustrates the NOEs between backbone C^{α} and amide protons on residues 19–29. Strong NOEs were observed between the C^{α} protons on residues 21 and 26 and also between the C^{α} protons on residues 19 and 29. Several other cross-strand NOEs are also illustrated in

Figure 8. Table II shows that short NH–NH distances were observed between residues 23 to 24 and residues 24 to 25. This pattern of d_{NN} connectivities is consistent with these residues being involved in a tight turn (Wagner et al., 1986). These results indicate that residues 19–29 in NP-5 form an antiparallel β-sheet and that this sheet has the hairpin structure schematically illustrated in Figure 8. The slowly exchanging amide protons on these residues are circled in the figure and are consistent with the pattern of cross-strand hydrogen bonding found in antiparallel β-sheet secondary structures. This β-sheet is the only secondary structure information that can be confidently obtained from qualitative analysis of these NOE data on NP-5. Quantitative interpretation of the proton–proton distances derived from NOE data is being used as input for a distance geometry algorithm to generate the complete three-dimensional structure of NP-5 in solution (A. C. Bach, II, D. Hare, and A. Pardi, unpublished results).

CONCLUSIONS

Essentially complete proton resonance assignment of the rabbit antimicrobial peptide NP-5 has been made from a variety of 2D NMR experiments. The application of several recently developed techniques such as isotropic mixing and triple-quantum experiments facilitated the assignment procedure in the molecule. The use of a solvent suppression NOESY pulse sequence and a double-quantum experiment allowed spectra to be acquired in 90% H_2O with no loss of $C^{\alpha}H$–NH cross-peaks near the water signal. By use of these procedures, resonance assignment of NP-5 was made from data taken at a single temperature. The ability to make complete assignments from 2D spectra at one temperature significantly reduces the already considerable amount of NMR time required for sequential resonance assignment in proteins.

A triple-quantum experiment proved extremely valuable for the assignment of the C^{α} and C^{β} protons in NP-5. The main advantage of this experiment is that cross-peaks occur at triple-quantum frequencies in ω_1. In contrast, for a triple-quantum-filtered COSY experiment (Piantini et al., 1982; Shaka & Freeman, 1983) cross-peaks occur at single-quantum frequencies in both the ω_1 and ω_2 dimensions. Thus, if cross-peaks from two three-spin systems overlap in a COSY or DQF-COSY spectrum, they will also overlap in the triple-quantum-filtered COSY experiment. However, these protons would be resolved in the TQ experiment as long as the spin systems have different triple-quantum frequencies. It is highly unlikely that all the single-quantum frequencies and both triple-quantum frequencies will be identical in the two spin systems. In addition, data obtained from a multiple-quantum 2D spectrum can be used to predict the location of cross-peaks in a single-quantum 2D spectrum. The results on NP-5 clearly show that the triple-quantum COSY experiment represents an extremely valuable technique for extending and confirming spin-system assignments made from single-quantum spectra. Therefore, we propose that TQ experiments should become a standard tool in the sequential assignment procedure of proteins. We also note that the combination of information from a number of complementary 2D NMR data sets (such as DQ, TQ, and TOCSY spectra in addition to DQF-COSY and NOESY spectra) not only accelerates the assignment process but also leads to a higher degree of confidence in the resonance assignments. Such combinations of complementary data will be extremely useful in the development of automated resonance assignment techniques in biopolymers.

Once complete resonance assignments have been made in a molecule, it is possible to identify NOEs originating from nonneighboring residues. This information is then used to generate the secondary and tertiary structure of the molecule. The NOESY spectra on NP-5 contain a large number of such "long-range" NOEs, and qualitative analysis of some of these NOEs shows the presence of an antiparallel β-sheet, in a hairpin conformation, involving residues 19–29. More detailed analysis of all the observed NOEs in NP-5 will be used to determine the full three-dimensional structure of this peptide in solution. The solution structure of NP-5 will then be compared with the structures of the homologous defensins NP-2 and HNP-1, obtained by X-ray crystallography (Westbrook et al., 1984). In addition to NP-5, we are also studying the defensins NP-2 and HNP-1 by 2D NMR. These three peptides possess various degrees of antibiotic, antiviral, and fungicidal activity, and the structural origins for these differences in biological activity is the subject of active investigation.

ACKNOWLEDGMENTS

We thank Dr. R. I. Lehrer (Department of Medicine, UCLA) for helpful discussions and Dr. D. Hare (Hare Research Inc.) for providing us with a copy of his 2D NMR processing software.

Registry No. NP-5, 108365-71-5.

REFERENCES

Bax, A., & Davis, D. G. (1985) *J. Magn. Reson. 65*, 355–360.
Billeter, M., Braun, W., & Wuethrich, K. (1982) *J. Mol. Biol. 155*, 321–346.
Bodenhausen, G. (1982) *Progr. Nucl. Magn. Reson. Spectrosc. 14*, 137–173.
Boyd, J., & Redfield, C. (1986) *J. Magn. Reson. 68*, 67–84.
Braunschweiler, L., & Ernst, R. R. (1983) *J. Magn. Reson. 53*, 521–528.
Bruenger, A. T., Clore, G. M., Gronenborn, A. M., & Karplus, M. (1986) *Proc. Natl. Acad. Sci. U.S.A. 83*, 3801–3805.
Bundi, A., & Wuethrich, K. (1979) *Biopolymers 18*, 285–297.
Davis, D. G., & Bax, A. (1985) *J. Am. Chem. Soc. 107*, 2820–2821.
Eich, G., Bodenhausen, G., & Ernst, R. R. (1982) *J. Am. Chem. Soc. 104*, 3731–3732.
Englander, S. W., & Kallenbach, N. R. (1984) *Q. Rev. Biophys. 16*, 521–655.
Guittet, E., Piveteau, D., Delsuc, M. A., & Lallemand, J. V. (1985) *J. Magn. Reson. 62*, 336–339.
Havel, T. F., & Wuethrich, K. (1985) *J. Mol. Biol. 182*, 281–294.
Hore, P. J. (1983) *J. Magn. Reson. 55*, 283–300.
Kaptein, R., Zuiderweg, E. R. P., Scheek, R. M., Boelens, R., & van Gunsteren, W. F. (1985) *J. Mol. Biol. 182*, 179–182.
Lehrer, R. I., Szklarek, D., Ganz, T., & Selsted, M. E. (1985a) *Infect. Immun. 49*, 207–211.
Lehrer, R. I., Szklarek, D., Ganz, T., & Selsted, M. E. (1985b) *J. Virol. 54*, 467–472.
Macura, S., & Ernst, R. R. (1980) *Mol. Phys. 41*, 95–117.
Marion, D., & Wuethrich, K. (1983) *Biochem. Biophys. Res. Commun. 113*, 967–974.
McDonald, C. C., & Phillips, W. D. (1969) *J. Am. Chem. Soc. 91*, 1513–1521.
Mueller, L., & Ernst, R. R. (1979) *Mol. Phys. 38*, 963–992.
Neuhaus, P., Wagner, G., Vasak, M., Kagi, H. R., & Wuethrich, K. (1985) *Eur. J. Biochem. 151*, 257–273.
Otting, G., & Wuethrich, K. (1983) *J. Magn. Reson. 66*, 359–363.
Otting, G., Widmer, H., Wagner, G., & Wuethrich, K. (1986) *J. Magn. Reson. 66*, 187–193.

Pardi, A., Wagner, G., & Wuethrich, K. (1983) *Eur. J. Biochem. 137*, 445–454.
Pardi, A., Billeter, M., & Wuethrich, K. (1984) *J. Mol. Biol. 180*, 741–751.
Piantini, U., Sorensen, O. W., & Ernst, R. R. (1982) *J. Am. Chem. Soc. 104*, 6800–6801.
Rance, M., & Wright, P. E. (1986) *J. Magn. Reson. 66*, 372–378.
Schwartz, A. L., & Cutnell, J. D. (1983) *J. Magn. Reson. 53*, 398–411.
Selsted, M. E., Szklarek, D., & Lehrer, R. I. (1984) *Infect. Immun. 45*, 150–154.
Selsted, M. E., Brown, D. M., DeLange, R. J., Harwig, S. S. L., & Lehrer, R. I. (1985a) *J. Biol. Chem. 260*, 4579–4584.
Selsted, M. E., Harwig, S. S. L., Ganz, T., Schilling, J. W., & Lehrer, R. I. (1985b) *J. Clin. Invest. 76*, 1436–1439.
Shaka, A. J., & Freeman, R. (1983) *J. Magn. Reson. 51*, 169–173.
States, D. J., Harberkorn, R. A., & Reuben, D. J. (1982) *J. Magn. Reson. 48*, 286–292.
Summers, M. F., Marzilli, L. G., & Bax, A. (1986) *J. Am. Chem. Soc. 108*, 4285–4294.
Wagner, G. (1983) *J. Magn. Reson. 55*, 151–156.
Wagner, G., & Wuethrich, K. (1982a) *J. Mol. Biol. 155*, 347–366.
Wagner, G., & Wuethrich, K. (1982b) *J. Mol. Biol. 160*, 343–361.
Wagner, G., & Zuiderweg, E. R. P. (1983) *Biochem. Biophys. Res. Commun. 113*, 854–860.
Wagner, G., Pardi, A., & Wuethrich, K. (1983) *J. Am. Chem. Soc. 105*, 5948–5949.
Wagner, G., Neuhaus, D., Worgotter, E., Vasak, M., Kagi, J. H. R., & Wuethrich, K. (1986) *J. Mol. Biol. 187*, 131–135.
Wand, A. J., Roder, H., & Englander, S. W. (1986) *Biochemistry 25*, 1107–1114.
Wemmer, D. E., & Kallenbach, N. R. (1983) *Biochemistry 22*, 1901–1906.
Westbrook, E. M., Lehrer, R. I., & Selsted, M. E. (1984) *J. Mol. Biol. 178*, 783–785.
Wider, G., Lee, K. H., & Wuethrich, K. (1982) *J. Mol. Biol. 155*, 367–388.
Wider, G., Hosur, R. V., & Wuethrich, K. (1983) *J. Magn. Reson. 52*, 130–135.
Williamson, M. P., Marion, D., & Wuethrich, K. (1984) *J. Mol. Biol. 173*, 341–359.
Williamson, M. P., Havel, T. F., & Wuethrich, K. (1985) *J. Mol. Biol. 182*, 295–315.
Wokaun, A., & Ernst, R. R. (1977) *Chem. Phys. Lett. 52*, 407–412.
Wuethrich, K., Wider, G., Wagner, G., & Braun, W. (1982) *J. Mol. Biol. 155*, 311–319.
Wuethrich, K., Billeter, M., & Braun, W. (1984) *J. Mol. Biol. 180*, 715–740.
Zuiderweg, E. R. P. (1986) *J. Magn. Reson. 66*, 153–156.
Zuiderweg, E. R. P., Kaptein, R., & Wuethrich, K. (1983) *Eur. J. Biochem. 137*, 279–293.

Sulfhydryl-Alkylating Reagents Inactivate the NAD Glycohydrolase Activity of Pertussis Toxin†

Harvey R. Kaslow* and David D. Lesikar
Department of Physiology and Biophysics, University of Southern California School of Medicine, Los Angeles, California 90033

Received November 10, 1986; Revised Manuscript Received March 6, 1987

ABSTRACT: The combination of ATP, CHAPS (3-[(3-cholamidopropyl)dimethylammonio]-1-propanesulfonate), and DTT (dithiothreitol) is known to promote the expression of the NAD glycohydrolase activity of pertussis toxin, which resides in the toxin's S1 subunit. By monitoring changes in electrophoretic mobility, we have found that ATP and CHAPS act by promoting the reduction of the disulfide bond of the S1 subunit. In addition, ATP, CHAPS, and DTT allowed sulfhydryl-alkylating reagents to inactivate the NAD glycohydrolase activity. In the presence of iodo[^{14}C]acetate, the combination of ATP, CHAPS, and DTT increased ^{14}C incorporation into only the S1 subunit of the toxin, indicating that alkylation of this subunit was responsible for the loss of activity. If iodoacetate is used as the alkylating reagent, alkylation can be monitored by an acidic shift in the isolectric point of the S1 peptide. Including NAD in alkylation reactions promoted the accumulation of a form of the S1 peptide with an isoelectric point intermediate between that of native S1 and that of S1 alkylated in the absence of NAD. This result suggests that NAD interacts with one of the two cysteines of the S1 subunit. In addition, we found the pH optimum for the NAD glycohydrolase activity of pertussis toxin is 8, which may reflect the participation of a cysteine in the catalytic mechanism of the toxin.

The bacterium *Bordetella pertussis* causes the disease whooping cough [for review, see Weiss and Hewlett (1986)]. Since the introduction of a "whole-cell" vaccine, consisting of killed *B. pertussis*, the incidence of the disease has declined dramatically. Unfortunately, this vaccine may cause severe adverse reactions (Fulginiti, 1984; Hinman & Koplan, 1984; Cody et al., 1981; Miller et al., 1984). *B. pertussis* produces several toxins, including one termed pertussis toxin, which is considered to be an important protective component of the vaccine (Munoz et al., 1981; Oda et al., 1983; Sato et al. 1981; Sato & Sato, 1984). Thus, in an attempt to minimize adverse

† This work was supported by grants from the NIH and by the Department of Physiology and Biophysics, University of Southern California School of Medicine.
* Address correspondence to this author.

0006-2960/87/0426-4397$01.50/0